

## Instrumentation for beam-foil spectroscopic studies in the UV-visible region

TAPAN NANDI, V NANAL, W A FERNANDES, C A DESAI, M B KURUP,  
K G PRASAD, P M R RAO\* and S PADMANABHAN\*

Tata Institute of Fundamental Research, Homi Bhabha Road, Bombay 400 005, India

\*Spectroscopy Division, Bhabha Atomic Research Centre, Bombay 400 085, India

MS received 19 August 1994

**Abstract.** A facility for carrying out beam-foil spectroscopic studies in the UV and visible region using the 400 kV electrostatic ion accelerator at Tata Institute of Fundamental Research, Bombay is described.

**Keywords.** Beam-foil spectroscopy; mean lifetimes; relative excitation function; IR telemetry; ion accelerator.

**PACS No.** 32.70

### 1. Introduction

The 400 kV positive ion accelerator [1] was recently re-installed at the Tata Institute of Fundamental Research with many modifications to improve its operation for various experiments like Beam-Foil Spectroscopy (BFS), Rutherford Back Scattering (RBS) and channeling, inner shell ionization, ion implantation, etc. Three beam lines have been installed to facilitate these measurements. The full operation of the accelerator is controlled by an infrared (IR) telemetry system designed and built indigenously. An inclined plate electrostatic deflector is used to direct the beam into any of the three beam lines. One of the beam lines is dedicated for BFS to study the properties of excited electronic states in atoms and ions [2]. In this paper we describe in detail the BFS set up in addition to the 400 kV accelerator and its control system.

In the BFS method, excited levels in neutral and ionized species are created by passing the energetic ion beam through a thin carbon foil. Electrons may be lost or excited during passage of ions through the foil, and additional electrons may be captured while the ions are emerging from the foil. After this electronic rearrangement the ion or atom is frequently left in a singly or multiply excited electronic configurations. Singly excited states may be low or high lying or Rydberg states while multiply excited states lie above the ionization limit. The latter can therefore autoionize. However, many of them are forbidden against autoionization and decay radiatively. Excited states decaying by the emission of photon can be detected using the technique of BFS which is a very useful method to gain insight into the properties of excited levels. The high lying, Rydberg and multiply excited states are not often populated in conventional photon sources. An added advantage is that BFS is suitable for measuring the lifetimes of these wide variety of states in neutral and ionized atoms in 10 ps to 100 ns range in a relatively simple way. This also enables one to measure quantum beats, Lamb shift, etc [2].

## 2. 400 kV ion accelerator

The schematic diagram of the 400 kV ion accelerator is shown in figure 1. A Neilsen type hot cathode penning ion source [3] is used. This ion source is capable of producing ions both from gaseous and solid materials. In the case of solid materials  $\text{CCl}_4$  or Ar is used as a supporting gas. Ions extracted by the extraction electrode (0–30 kV) are focused by an Einzel lens and are then analyzed for isotopic purity by a  $90^\circ$  analyzing magnet, having rigidity of 4000 Gm, before the main acceleration. The maximum acceleration voltage of 400 kV is achieved using the Danfysik high frequency multidoubler type high voltage power supply. The ion source, ion extractor, Einzel lens, the mass analyzing magnet and associated electronics together with the turbomolecular pumping system operate at this terminal voltage. The required AC power to operate these components is provided by a motor-generator set, with the generator floating at the terminal voltage. The motor is coupled to the generator using an insulating PVC shaft.

The pumping system was designed to achieve vacuum better than  $1 \times 10^{-5}$  torr in the entire pre-acceleration region. Three beam lines were set up at  $0^\circ$ ,  $+12^\circ$  and  $-12^\circ$  with respect to the initial beam direction. Using a pair of inclined ( $8^\circ$ ) electrostatic deflection plates [4] the accelerated beam could be switched to any one of these three lines. The inclined plate geometry was adopted to facilitate larger bending by using comparatively smaller voltages than that required in the case of parallel plates for the same incident beam condition. After acceleration the beam may be focused with the electrostatic quadrupole lens before entering the deflector.

The wireless telemetry system for the 400 kV accelerator is based on infra-red transmitter-receiver diode pair which are robust and readily available. Remote control operation using the infra-red link offers some advantages such as lower spurious radiation and less interference from multiple reflections. The IR telemetry system is

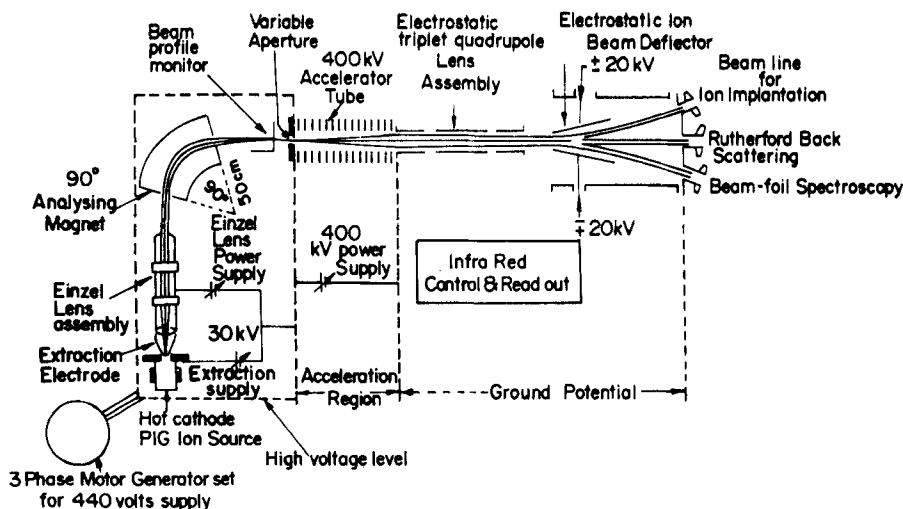


Figure 1. A schematic diagram of the 400 kV heavy ion accelerator at TIFR. The ion source is kept at 15 kV above the dome potential. Hence its control and read out connections are isolated from the dome using fibre optic cables.

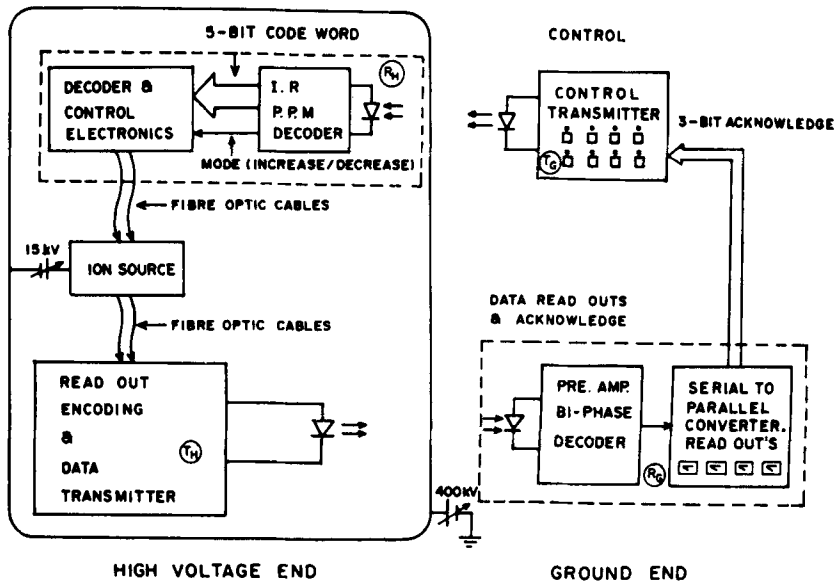


Figure 2. A schematic diagram of the infra-red telemetry system to control, monitor and optimize the operation of the 400 kV heavy ion accelerator at TIFR.

divided into two parts (figure 2) each consisting of a transmitter and a receiver. The control transmitter at the ground end ( $T_G$ ) controls the parameters at the high voltage end. The transmitter  $T_H$  at high voltage end transmits the set values of parameters to the ground side which are read by the receiver  $R_G$  and are displayed on panel meters.

The control transmitter ( $T_G$ ) operates different parameters through a matrix of switches. Each parameter has been assigned a code word which is transmitted using a Pulse Position Modulated (PPM) code. In PPM code, the time interval between the two pulses is different for '1', '0' and 'stop' bits. The relation between '1', '0', and 'stop' intervals in the transmitted pulse is set to the standard value of 2:3:6. Each code word is 5-bits in length and hence we can control 32 parameters. A carrier of 36 kHz is normally inserted in the 5 bit code word to distinguish between the noise and signal. This word is received at the high voltage end by a PIN photodiode ( $R_H$ ) where PPM signal is amplified and decoded properly in order to control the particular parameter. The parameters controlled are: ion source filament current, gas pressure, source magnet current, anode voltage, extraction voltage, lens voltage and the analyzing magnet current. The transmitter at the high voltage end ( $T_H$ ) transmits each parameter (channel) in digital form, having 8 or 12 bits depending on the resolution required. These parameter values are sent in a bi-phase format to eliminate interference from extraneous IR sources. All parameters are sent sequentially and serially along with the Sync word and acknowledge bits using time division multiplexing (TDM). The sync word locks the transmitter and receiver clocks to ensure proper decoding by the receiver. The receiver at ground end separates each channel and displays corresponding parameter on pre assigned meter. The acknowledge bits are decoded to illuminate the appropriate LED on the control panel to indicate the parameter that is being controlled.

### 3. The beam-foil chamber and spectrometer

The dedicated beam line made of stainless steel for the beam-foil spectroscopic studies consists of a pumping cross with a closed cycle cryopump, a continuously variable double slit collimator and an electrically insulated target chamber which also serves as a deep Faraday cup. The variable collimator ( $0\text{--}100\text{ mm}^2$ ) consists of two diamond shaped openings of  $1\text{ cm} \times 1\text{ cm}$  made diametrically opposite to each other on a hollow cylinder of 40 mm diameter. The beam size can be varied by simply rotating this cylinder along its axis which is perpendicular to the beam axis. The beam-foil target chamber is basically a cross of 100 mm diameter tubes. A schematic diagram of the chamber along with the beam line is shown in figure 3. The cross has two 50 mm diameter asymmetric ports perpendicular to the beam axis. This asymmetry facilitates the foil traversal of 80 mm upstream along the beam path for lifetime measurements. One of these two ports has a quartz window to enable light emitted by the excited ions to be transmitted to the spectrometer. At the end of the chamber, there is a NaCl coated glass window which acts as a view port. Because of large scattering angle of ions at low energy [5], the scattered particles can hit the chamber walls easily and consequently the secondary electron suppression becomes very important in charge measurements. Therefore the entire target chamber is isolated from the rest of the beam line and is used as Faraday cup. At the entrance of the chamber there is a provision for electrostatic suppression of secondary electrons. The target holder is mounted from the top of the chamber using Wilson seal arrangement. This target ladder can hold up to ten foils at a time. Special care has been taken in designing the target ladder so that it does not block any light emitted by the excited ions as they emerge from the foil.

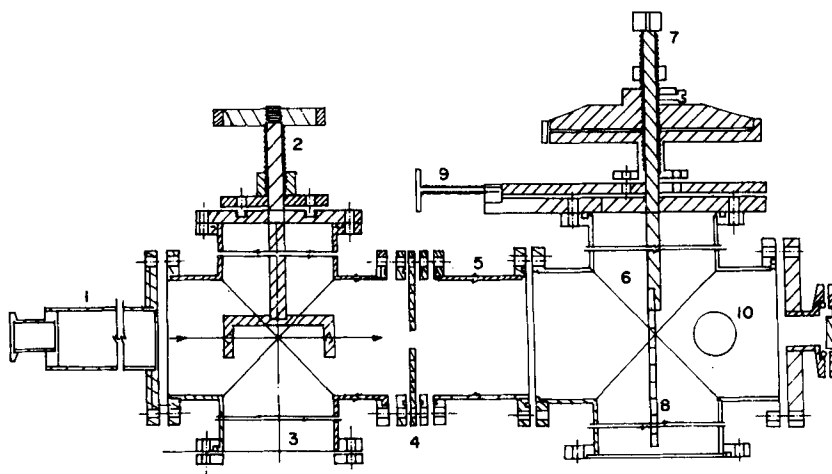


**Figure 3.** A schematic diagram of a dedicated beam line and the target chamber (not to the scale) for beam-foil spectroscopy experiment in the UV-visible range: (1) a drift tube (2) a variable ( $0\text{--}100\text{ mm}^2$ ) collimator, (3) a pumping port for a closed cycle cryopump, (4) electron suppressor, (5) another drift tube as a part of the Faraday cup, (6) the target chamber cum Faraday cup, (7) target manipulator with 3-degrees of freedom, (8) the target ladder capable of holding eleven targets and also avoids shadowing due to the frame, (9) an arrangement for translational movement of the target holder along the beam direction, and (10) quartz window for the light detection.

### Beam-foil spectroscopic studies

The target ladder can be tilted to any angle with respect to the beam direction about the vertical axis. Its lateral movement in the vacuum is controlled by a guided screw of a fine pitch with a precision of 0.025 mm. This movement is measured by a vernier scale attached parallel to the beam axis on the top flange. The entire target chamber is evacuated by a cryopump to obtain hydrocarbon free vacuum of the order of  $1 \times 10^{-6}$  torr or better. This has helped greatly in reducing foil deterioration during the measurements. Carbon foils of thickness  $4\text{--}5 \mu\text{g}/\text{cm}^2$  were prepared by cracking ethylene gas under DC discharge [6].

Radiation emitted from the ions excited while passing through the foil is recorded in a direction perpendicular to the beam downstream from the foil. A quartz lens is used to focus, with unity magnification, the emitted radiation onto the entrance slit of a 0.45 m monochromator (Pacific precision instruments Co.) having a Czerny-Turner mount as shown in figure 4. This monochromator is equipped with a 1180 grooves/mm grating blazed at  $3000 \text{ \AA}$  having a linear dispersion of  $16 \text{ \AA}/\text{mm}$ . The widths of the entrance and exit slits of the monochromator were fixed at  $200 \mu\text{m}$ . The entire optical system was aligned to achieve highest resolution and efficiency. The monochromator was calibrated with standard sources like mercury lamp and iron hollow cathode discharge tube which showed that the system could resolve spectral lines of less than  $2 \text{ \AA}$  separation. The overall resolution of the spectrometer becomes slightly worse when we use the beam foil source. This is caused by the Doppler broadening due to the finite acceptance angle of the spectrometer and second order Doppler shift. The wavelength dispersed photons were detected by a thermoelectrically cooled photomultiplier operated in the single-photon counting mode. The background without the beam was usually about 0.5 count/sec. The relative efficiency of the spectrometer is measured using a mercury lamp and is shown in figure 5. A multichannel scalar (MCS) based on 8085 microprocessor ( $\mu\text{P}$ ) [7] is used to record the spectrum. The signal from the photon detector is amplified and fed to a pulse height discriminator whose digital output is counted in a 4 stage binary counter. The

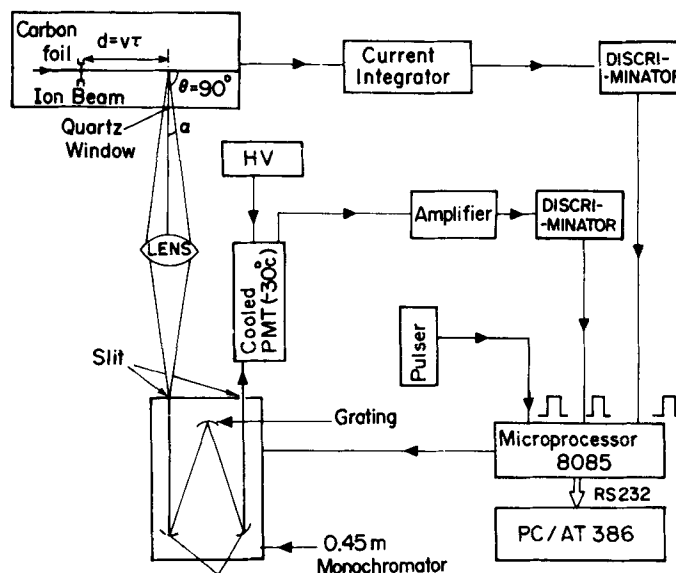


**Figure 4.** A block diagram of the data processing system for beam-foil spectroscopy experiment in the UV-visible range.

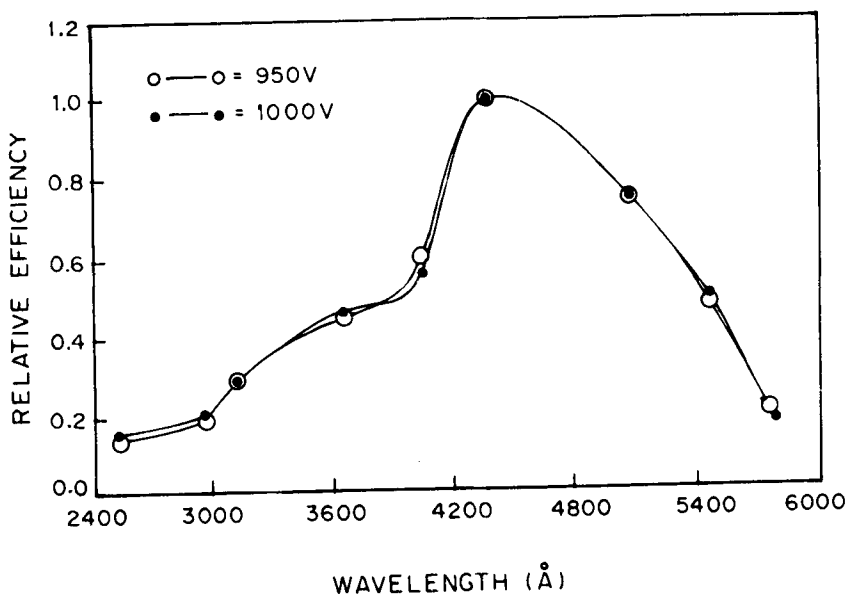


**Figure 5.** The relative efficiency curve for a spectrometer in the UV-visible range at two different high voltages applied to photo cathode of the photomultiplier tube.

wavelength setting of the monochromator is changed with the help of a built in stepper motor, which also is controlled by the microprocessor. The range of wavelength over which the spectrum is to be recorded, the step size ( $\delta\lambda$ ) and number of normalizing pulses (from the current integrator) for which data is to be collected at each step are supplied as input parameters to the microprocessor. The  $\mu\text{P}$  generates a signal to move the motor which in turn changes the monochromator setting by the preset step size  $\delta\lambda$ . The  $\mu\text{P}$  then gives the signal to reset the counter and start the photon counting. The digital output of the current integrator is counted in a separate counter. When this count reaches the preset value, the photon counting is stopped and the reading is stored in the memory. Memory address is then incremented to the next value and the monochromator setting is changed. This process is continued till the final preset value of the wavelength range is reached. While data are being collected at a given setting, the recorded spectrum is displayed on the oscilloscope. The system has the facility for accepting inputs from two detectors. To take care of beam current instability, time taken for data collection at each wavelength is also recorded. This is done by counting pulses from a standard pulse generator and is used for proper background subtraction. The data are then transferred to a PC through RS232 serial link for further analysis.

#### 4. Data collection and analysis

Two typical beam foil spectra one each of Na ions and Ar ions passing through carbon foil are shown in figure 6. The wavelength of the respective lines are indicated in the figure. Further, the charge state of the ion from which the spectral line originates is also shown against each line. It should be noted that lines from a number of ionic states are present in the beam foil spectra. Usually, the charge state of the de-exciting ion can be determined by measuring the excitation function, i.e. by observing the

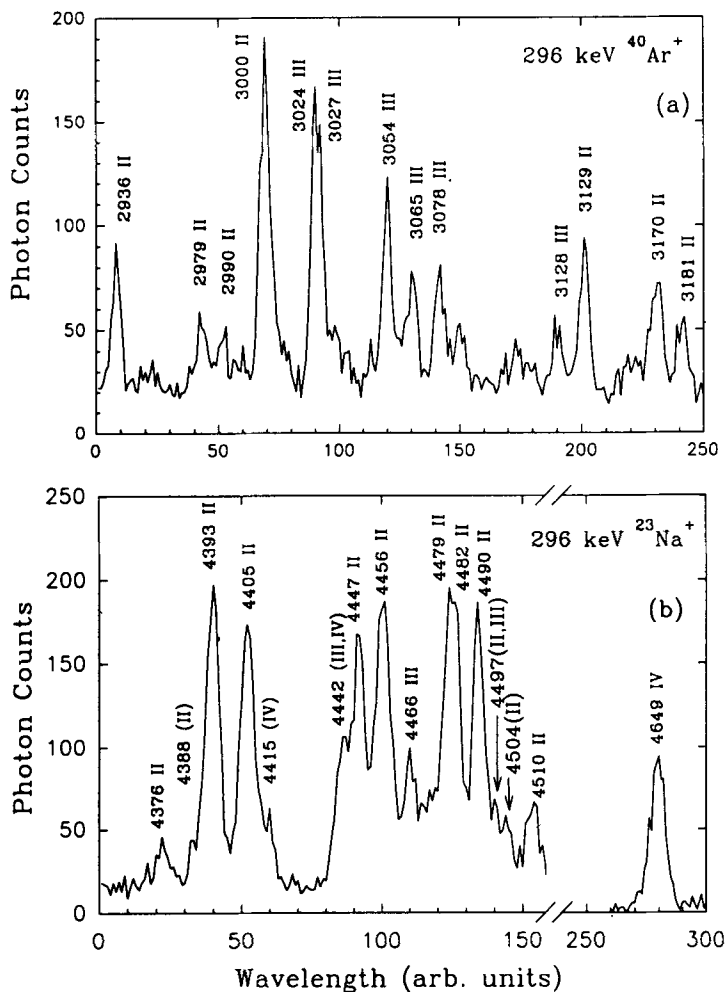


**Figure 6.** Beam-foil spectra of 296 keV (a)  $\text{Ar}^+$  ions in the wave length range 2390–3190 Å/ and (b)  $\text{Na}^+$  ions in the wave length range 4360–4660 Å/ and passing through a  $5 \mu\text{g}/\text{cm}^2$  carbon foil. The charge state corresponding to the parent ions from which the transitions take place is shown along side the wavelength.

intensity of the photons as a function of energy of the incident ions. In order to get the excitation function curves, the population  $N_i$  of level  $i$ , is calculated from the yield  $S_{ij}$  of the de-exciting optical transition (from level  $i$  to level  $j$ ) of wavelength  $\lambda_{ij}$  in the usual way from the expression [8],

$$N_i = \frac{4\pi S_{ij} v}{\Omega K_{ij} A_{ij} I \Delta l} \quad (1)$$

where  $K_{ij}$  is the quantum efficiency of the detection system for wavelength  $\lambda_{ij}$ ,  $\Delta l$  is the width of the observation region (which is kept constant) in the direction of the projectile,  $\Omega$  is the solid-angle subtended at the monochromator by the effective optical source and  $I$  is the incident projectile flux. The velocity  $v$  of the projectile after emerging from the foil is estimated from the post foil energy,  $E_{\text{postfoil}} = E_{\text{inc}} - E_{\text{loss}}$

( $E_{\text{loss}}$  can be estimated from the program TRIM90 [9]), using the following non-relativistic expression

$$v = 0.4397(E_{\text{postfoil}}(\text{keV})/M(\text{amu}))^{1/2} \times 10^8 \text{ cm/sec.} \quad (2)$$

The quantity  $A_{ij}$  is the transition probability for  $\lambda_{ij}$ . As knowledge of  $A_{ij}$  is lacking in many cases, only relative level populations,

$$P_i = S_{ij}v/I \quad (3)$$

have been estimated in our investigation. Further, for comparison, these  $P_i$ 's are normalized at a certain incident ion energy. A typical relative excitation function curve along with the known relative charge state distribution [10] with incident ion energy is shown in figure 7. It may be seen from this figure that the normalized excitation behaviour closely follows the charge state distribution. This agreement is better for higher ionic states.

For the lifetime measurements the time of flight method is usually used. In this method the distance of the foil from the entrance slit of the spectrometer is varied and the respective photon counts are observed to record an intensity decay curve for extracting the mean lifetime. The data are recorded upto a length for which the

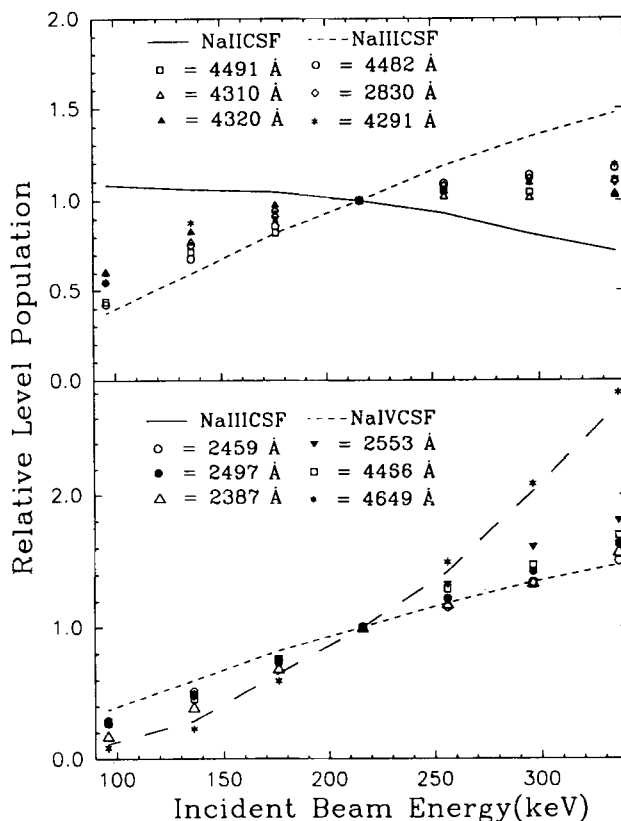
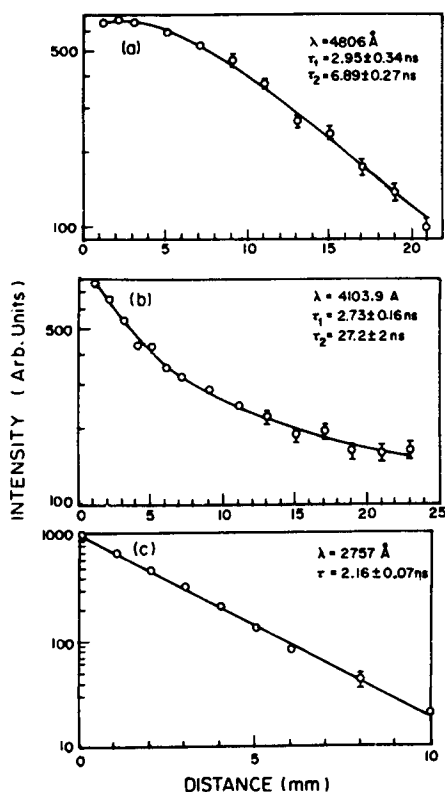


Figure 7. Relative excitation function curves observed for the various transitions from highly excited levels in Na II-IV. The overall uncertainty on each point is about 20%. CSF indicates the corresponding charge state fractions [10].





**Figure 8.** Decay curves for the measurement of lifetimes of (a)  $4p^4P_{5/2}$  level in Ar II, (b)  $5s^4P_{5/2}$  level in Ar II, (c)  $4p^2P_{7/2}^0$  level in Ar IV. The cascading effects are clearly visible in (a) and (b), where  $\tau_2$  is the lifetime of the feeding level.

observed counts fall close to the background. The width of the beam-foil light viewed by the spectrometer,  $dx$ , should be very small compared to the decay length of a level  $\nu t$ . As mentioned earlier, this short observation window is obtained by using an adjustable slit at the focal point of a unity magnification optical system. Since in the beam-foil excitation, levels higher than the one that is of the interest can also be populated, the experimentally observed decay curve is usually a sum of several exponentials due to 'feeding in' and 'cascading effects'. However, in most of the cases one to three exponential components give a very good estimate of the primary lifetime. Usually different numerical methods are employed in order to fit a multiexponential function to the experimental decay curve. We have extracted lifetimes by fitting a multiexponential function using the Levenberg-Marquardt method for non-linear least square fit which is a standard library routine in the CYBER computer at TIFR. Typical time of flight spectra with and without cascading effects are shown in figure 8.

Using this set-up detailed spectroscopic studies in systems like C, Na, Mg and Ar have been carried out [11–14] and many interesting results have been obtained.

## 5. Acknowledgements

The authors acknowledge Dr G Krishnamurthy for the valuable guidance and discussions while setting up the experimental facilities. One of us (TN) is highly

grateful to Dr R G Pillay for his invaluable advice in developing the electrostatic ion beam deflector. Authors are thankful to Mr D C Ephraim for making carbon foils and Central Workshop staff for building all the vacuum components. The help from S S Chauhan at all stages of instrumentation is acknowledged.

## References

- [1] R P Sharma, *Phys. News (India)* **7**, 110 (1976)
- [2] I Martinson, *Rep. Prog. Phys.* **52**, 152 (1989)
- [3] K O Neilsen, *Nucl. Instrum. Methods* **1**, 289 (1957)
- [4] Tapan Nandi, M B Kurup and K G Prasad, *DAE Symp. in Nucl. Phys. (India)* **B36**, 400 (1993)
- [5] H G Berry, *Rep. Prog. Phys.* **40**, 155 (1977)
- [6] G Dollinger and P Maier-Komor, *Nucl. Instrum. Methods* **A282**, 223 (1989)
- [7] Vandana Nanal, M B Kurup and K G Prasad, *DAE Symp. in Nucl. Phys. (India)* **B33**, 323 (1990)
- [8] B Andresen, S B Jensen, P S Ramanujam and E Veje, *Phys. Scr.* **20**, 65 (1979)
- [9] J F Ziegler and J P Biersack, *The stopping and range of ions in solids* (Pergamon Press, NY 1990)
- [10] P Hvelplund, E Laegsgaard, J O Olsen and S E Harris, *Nucl. Instrum Methods* **90**, 272 (1970)
- [11] Tapan Nandi, M B Kurup, K G Prasad and P M R Rao, *J. Phys.* **B27**, 1975 (1994)
- [12] Tapan Nandi, M B Kurup, K G Prasad, P M R Rao, S Padmanabhan, G Krishnamurthy, and A P Misra, *J. Quant. Spectrosc. Radiat. Transfer* **49**, 389 (1993)
- [13] Tapan Nandi, M B Kurup and K G Prasad, *Natl. Conf. on current trends in atomic and molecular physics (India) CURTAMP* **93**, 170 (1993)
- [14] B N Rajashekhar, P M R Rao, S Padmanabhan, M Jagdeesh, M B Kurup and K G Prasad, *Natl. Conf. on current trends in atomic and molecular physics (India) CURTAMP* **93**, 172 (1993)